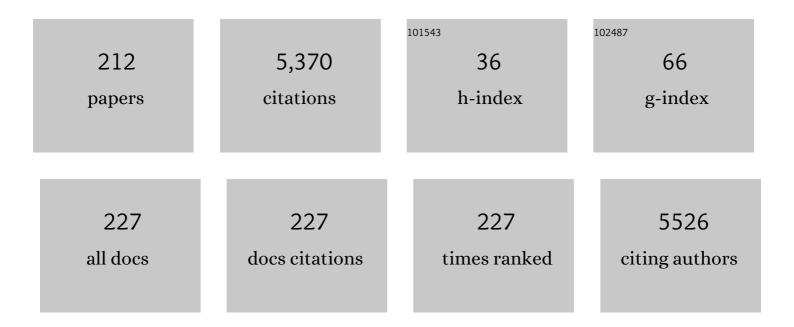
Marcus Carlsson

List of Publications by Year in descending order

Source: https://exaly.com/author-pdf/6931747/publications.pdf Version: 2024-02-01



#	Article	IF	CITATIONS
1	Design and validation of Segment - freely available software for cardiovascular image analysis. BMC Medical Imaging, 2010, 10, 1.	2.7	725
2	A Pilot Study of Rapid Cooling by Cold Saline and Endovascular Cooling Before Reperfusion in Patients With ST-Elevation Myocardial Infarction. Circulation: Cardiovascular Interventions, 2010, 3, 400-407.	3.9	223
3	Atrioventricular plane displacement is the major contributor to left ventricular pumping in healthy adults, athletes, and patients with dilated cardiomyopathy. American Journal of Physiology - Heart and Circulatory Physiology, 2007, 292, H1452-H1459.	3.2	207
4	Rapid Endovascular Catheter Core Cooling Combined With Cold Saline as an Adjunct toÂPercutaneous Coronary Intervention for theÂTreatment of Acute Myocardial Infarction. Journal of the American College of Cardiology, 2014, 63, 1857-1865.	2.8	203
5	Myocardium at Risk After Acute Infarction in Humans on Cardiac Magnetic Resonance. JACC: Cardiovascular Imaging, 2009, 2, 569-576.	5.3	184
6	The quantitative relationship between longitudinal and radial function in left, right, and total heart pumping in humans. American Journal of Physiology - Heart and Circulatory Physiology, 2007, 293, H636-H644.	3.2	158
7	Effect of intravenous TRO40303 as an adjunct to primary percutaneous coronary intervention for acute ST-elevation myocardial infarction: MITOCARE study results. European Heart Journal, 2015, 36, 112-119.	2.2	154
8	Quantification of left and right ventricular kinetic energy using four-dimensional intracardiac magnetic resonance imaging flow measurements. American Journal of Physiology - Heart and Circulatory Physiology, 2012, 302, H893-H900.	3.2	117
9	Vortex Ring Formation in the Left Ventricle of the Heart: Analysis by 4D Flow MRI and Lagrangian Coherent Structures. Annals of Biomedical Engineering, 2012, 40, 2652-2662.	2.5	114
10	Fully quantitative cardiovascular magnetic resonance myocardial perfusion ready for clinical use: a comparison between cardiovascular magnetic resonance imaging and positron emission tomography. Journal of Cardiovascular Magnetic Resonance, 2016, 19, 78.	3.3	110
11	Total heart volume variation throughout the cardiac cycle in humans. American Journal of Physiology - Heart and Circulatory Physiology, 2004, 287, H243-H250.	3.2	106
12	Quantification and visualization of cardiovascular 4D velocity mapping accelerated with parallel imaging or k-t BLAST: head to head comparison and validation at 1.5 T and 3 T. Journal of Cardiovascular Magnetic Resonance, 2011, 13, 55.	3.3	91
13	Relation between cardiac dimensions and peak oxygen uptake. Journal of Cardiovascular Magnetic Resonance, 2010, 12, 8.	3.3	85
14	Cardiac output and cardiac index measured with cardiovascular magnetic resonance in healthy subjects, elite athletes and patients with congestive heart failure. Journal of Cardiovascular Magnetic Resonance, 2012, 14, 51.	3.3	77
15	Left ventricular fluid kinetic energy time curves in heart failure from cardiovascular magnetic resonance 4D flow data. Journal of Cardiovascular Magnetic Resonance, 2015, 17, 111.	3.3	76
16	Vortex ring behavior provides the epigenetic blueprint for the human heart. Scientific Reports, 2016, 6, 22021.	3.3	69
17	A new automatic algorithm for quantification of myocardial infarction imaged by late gadolinium enhancement cardiovascular magnetic resonance: experimental validation and comparison to expert delineations in multi-center, multi-vendor patient data. Journal of Cardiovascular Magnetic Resonance. 2016. 18. 27.	3.3	67
18	Reduced administered activity, reduced acquisition time, and preserved image quality for the new CZT camera. Journal of Nuclear Cardiology, 2013, 20, 38-44.	2.1	62

#	Article	IF	CITATIONS
19	Contrast-Enhanced CMR Overestimates Early Myocardial Infarct Size. JACC: Cardiovascular Imaging, 2015, 8, 1379-1389.	5.3	55
20	Therapeutic Hypothermia for the Treatment of Acute Myocardial Infarction–Combined Analysis of the RAPID MI-ICE and the CHILL-MI Trials. Therapeutic Hypothermia and Temperature Management, 2015, 5, 77-84.	0.9	54
21	Quantification of left and right atrial kinetic energy using four-dimensional intracardiac magnetic resonance imaging flow measurements. Journal of Applied Physiology, 2013, 114, 1472-1481.	2.5	53
22	Evaluation of left ventricular volumes and ejection fraction by automated gated myocardial SPECT versus cardiovascular magnetic resonance. Clinical Physiology and Functional Imaging, 2005, 25, 135-141.	1.2	49
23	Quantitative MR measurements of regional and global left ventricular function and strain after intramyocardial transfer of VM202 into infarcted swine myocardium. American Journal of Physiology - Heart and Circulatory Physiology, 2008, 295, H522-H532.	3.2	49
24	Noninvasive Quantification of Pressure-Volume Loops From Brachial Pressure and Cardiovascular Magnetic Resonance. Circulation: Cardiovascular Imaging, 2019, 12, e008493.	2.6	49
25	Myocardial Microinfarction after Coronary Microembolization in Swine: MR Imaging Characterization. Radiology, 2009, 250, 703-713.	7.3	48
26	Multi-vendor, multicentre comparison of contrast-enhanced SSFP and T2-STIR CMR for determining myocardium at risk in ST-elevation myocardial infarction. European Heart Journal Cardiovascular Imaging, 2016, 17, 744-753.	1.2	47
27	Left and right ventricular hemodynamic forces in healthy volunteers and elite athletes assessed with 4D flow magnetic resonance imaging. American Journal of Physiology - Heart and Circulatory Physiology, 2017, 312, H314-H328.	3.2	45
28	Disturbed left and right ventricular kinetic energy in patients with repaired tetralogy of Fallot: pathophysiological insights using 4D-flow MRI. European Radiology, 2018, 28, 4066-4076.	4.5	45
29	Restrictive right ventricular physiology after Tetralogy of Fallot repair is associated with fibrosis of the right ventricular outflow tract visualized on cardiac magnetic resonance imaging. European Heart Journal Cardiovascular Imaging, 2013, 14, 978-985.	1.2	44
30	Manual correction of semi-automatic three-dimensional echocardiography is needed for right ventricular assessment in adults; validation with cardiac magnetic resonance. Cardiovascular Ultrasound, 2012, 10, 1.	1.6	43
31	Cardiovascular magnetic resonance of the myocardium at risk in acute reperfused myocardial infarction: comparison of T2-weighted imaging versus the circumferential endocardial extent of late gadolinium enhancement with transmural projection. Journal of Cardiovascular Magnetic Resonance, 2010, 12, 18,	3.3	42
32	Whole-heart four-dimensional flow can be acquired with preserved quality without respiratory gating, facilitating clinical use: a head-to-head comparison. BMC Medical Imaging, 2015, 15, 20.	2.7	42
33	Peak CKMB and cTnT accurately estimates myocardial infarct size after reperfusion. Scandinavian Cardiovascular Journal, 2007, 41, 44-50.	1.2	41
34	Effects of oxygen inhalation on cardiac output, coronary blood flow and oxygen delivery in healthy individuals, assessed with MRI. European Journal of Emergency Medicine, 2011, 18, 25-30.	1.1	41
35	Validation and reproducibility of cardiovascular 4D-flow MRI from two vendors using 2 × 2 parallel imaging acceleration in pulsatile flow phantom and inÂvivo with and without respiratory gating. Acta Radiologica, 2019, 60, 327-337.	1.1	41
36	Cardiovascular Magnetic Resonance to Predict Appropriate Implantable Cardioverter Defibrillator Therapy in Ischemic and Nonischemic Cardiomyopathy Patients Using Late Gadolinium Enhancement Border Zone. Circulation: Cardiovascular Imaging, 2017, 10, .	2.6	39

#	Article	IF	CITATIONS
37	The relationship between longitudinal, lateral, and septal contribution to stroke volume in patients with pulmonary regurgitation and healthy volunteers. American Journal of Physiology - Heart and Circulatory Physiology, 2014, 306, H895-H903.	3.2	38
38	Independent validation of fourâ€dimensional flow MR velocities and vortex ring volume using particle imaging velocimetry and planar laserâ€Induced fluorescence. Magnetic Resonance in Medicine, 2016, 75, 1064-1075.	3.0	35
39	Time-resolved tracking of the atrioventricular plane displacement in Cardiovascular Magnetic Resonance (CMR) images. BMC Medical Imaging, 2017, 17, 19.	2.7	35
40	Intracardiac 4D Flow MRI in Congenital Heart Disease: Recommendations on Behalf of the ISMRM Flow & Motion Study Group. Journal of Magnetic Resonance Imaging, 2019, 50, spcone.	3.4	35
41	Magnetic resonance imaging as a potential gold standard for infarct quantification. Journal of Electrocardiology, 2008, 41, 614-620.	0.9	34
42	Myocardium at risk by magnetic resonance imaging: head-to-head comparison of T2-weighted imaging and contrast-enhanced steady-state free precession. European Heart Journal Cardiovascular Imaging, 2012, 13, 1008-1015.	1.2	34
43	Effect of oxygen therapy on myocardial salvage in ST elevation myocardial infarction: the randomized SOCCER trial. European Journal of Emergency Medicine, 2018, 25, 78-84.	1.1	34
44	Validation and Development of a New Automatic Algorithm for Time-Resolved Segmentation of the Left Ventricle in Magnetic Resonance Imaging. BioMed Research International, 2015, 2015, 1-12.	1.9	33
45	Intracardiac 4D Flow MRI in Congenital Heart Disease: Recommendations on Behalf of the ISMRM Flow & Motion Study Group. Journal of Magnetic Resonance Imaging, 2019, 50, 677-681.	3.4	32
46	Blood flow imaging by optimal matching of computational fluid dynamics to 4Dâ€flow data. Magnetic Resonance in Medicine, 2020, 84, 2231-2245.	3.0	32
47	Magnetic resonance imaging quantification of left ventricular dysfunction following coronary microembolization. Magnetic Resonance in Medicine, 2009, 61, 595-602.	3.0	31
48	Heterogeneous Microinfarcts Caused by Coronary Microemboli: Evaluation with Multidetector CT and MR Imaging in a Swine Model. Radiology, 2010, 254, 718-728.	7.3	31
49	Moderate intensity supine exercise causes decreased cardiac volumes and increased outer volume variations: a cardiovascular magnetic resonance study. Journal of Cardiovascular Magnetic Resonance, 2013, 15, 96.	3.3	31
50	Combined preoperative information using a bullseye plot from speckle tracking echocardiography, cardiac CT scan, and MRI scan: targeted left ventricular lead implantation in patients receiving cardiac resynchronization therapy. European Heart Journal Cardiovascular Imaging, 2014, 15, 523-531.	1.2	31
51	Sample Size in Clinical Cardioprotection Trials Using Myocardial Salvage Index, Infarct Size, or Biochemical Markers as Endpoint. Journal of the American Heart Association, 2016, 5, e002708.	3.7	31
52	Cardiac Resynchronization Therapy Guided by Echocardiography, MRI, and CT Imaging. JACC: Clinical Electrophysiology, 2020, 6, 1300-1309.	3.2	31
53	Decreased Diastolic Ventricular Kinetic Energy in Young Patients with Fontan Circulation Demonstrated by Four-Dimensional Cardiac Magnetic Resonance Imaging. Pediatric Cardiology, 2017, 38, 669-680.	1.3	30
54	Variable velocity encoding in a threeâ€dimensional, threeâ€directional phase contrast sequence: Evaluation in phantom and volunteers. Journal of Magnetic Resonance Imaging, 2012, 36, 1450-1459.	3.4	28

#	Article	IF	CITATIONS
55	A comparison between radial strain evaluation by speckle-tracking echocardiography and cardiac magnetic resonance imaging, for assessment of suitable segments for left ventricular lead placement in cardiac resynchronization therapy. Europace, 2014, 16, 1779-1786.	1.7	27
56	Hemodynamic forces using four-dimensional flow MRI: an independent biomarker of cardiac function in heart failure with left ventricular dyssynchrony?. American Journal of Physiology - Heart and Circulatory Physiology, 2018, 315, H1627-H1639.	3.2	27
57	Quantifying coronary sinus flow and global LV perfusion at 3T. BMC Medical Imaging, 2009, 9, 9.	2.7	26
58	Decreased global myocardial perfusion at adenosine stress as a potential new biomarker for microvascular disease in systemic sclerosis: a magnetic resonance study. BMC Cardiovascular Disorders, 2018, 18, 16.	1.7	26
59	Volume Tracking: A new method for quantitative assessment and visualization of intracardiac blood flow from three-dimensional, time-resolved, three-component magnetic resonance velocity mapping. BMC Medical Imaging, 2011, 11, 10.	2.7	25
60	Quantitative polar representation of left ventricular myocardial perfusion, function and viability using SPECT and cardiac magnetic resonance: initial results. Clinical Physiology and Functional Imaging, 2005, 25, 215-222.	1.2	24
61	Submaximal adenosineâ€induced coronary hyperaemia with 12Âh caffeine abstinence: implications for clinical adenosine perfusion imaging tests. Clinical Physiology and Functional Imaging, 2015, 35, 49-56.	1.2	24
62	Altered biventricular hemodynamic forces in patients with repaired tetralogy of Fallot and right ventricular volume overload because of pulmonary regurgitation. American Journal of Physiology - Heart and Circulatory Physiology, 2018, 315, H1691-H1702.	3.2	24
63	Hemodynamic forces in the left and right ventricles of the human heart using 4D flow magnetic resonance imaging: Phantom validation, reproducibility, sensitivity to respiratory gating and free analysis software. PLoS ONE, 2018, 13, e0195597.	2.5	24
64	The endocardial extent of reperfused first-time myocardial infarction is more predictive of pathologic Q waves than is infarct transmurality: a magnetic resonance imaging study. Clinical Physiology and Functional Imaging, 2007, 27, 101-108.	1.2	23
65	Semi-automatic segmentation of myocardium at risk in T2-weighted cardiovascular magnetic resonance. Journal of Cardiovascular Magnetic Resonance, 2012, 14, 20.	3.3	22
66	Experimental validation of contrast-enhanced SSFP cine CMR for quantification of myocardium at risk in acute myocardial infarction. Journal of Cardiovascular Magnetic Resonance, 2016, 19, 12.	3.3	22
67	Importance of standardizing timing of hematocrit measurement when using cardiovascular magnetic resonance to calculate myocardial extracellular volume (ECV) based on pre- and post-contrast T1 mapping. Journal of Cardiovascular Magnetic Resonance, 2018, 20, 46.	3.3	22
68	The Effects of Oxygen Therapy on Myocardial Salvage in ST Elevation Myocardial Infarction Treated with Acute Percutaneous Coronary Intervention: The Supplemental Oxygen in Catheterized Coronary Emergency Reperfusion (SOCCER) Study. Cardiology, 2015, 132, 16-21.	1.4	21
69	Multicenter Consistency Assessment of Valvular Flow Quantification With AutomatedÂValve Tracking in 4D Flow CMR. JACC: Cardiovascular Imaging, 2021, 14, 1354-1366.	5.3	21
70	Young patients with hypertrophic cardiomyopathy, but not subjects at risk, show decreased myocardial perfusion reserve quantified with CMR. European Heart Journal Cardiovascular Imaging, 2014, 15, 1350-1357.	1.2	20
71	Regional Stress-Induced Ischemia in Non-fibrotic Hypertrophied Myocardium in Young HCM Patients. Pediatric Cardiology, 2015, 36, 1662-1669.	1.3	20
72	Extent of Myocardium at Risk for Left Anterior Descending Artery, Right Coronary Artery, and Left Circumflex Artery Occlusion Depicted by Contrast-Enhanced Steady State Free Precession and T2-Weighted Short Tau Inversion Recovery Magnetic Resonance Imaging. Circulation: Cardiovascular Imaging, 2016, 9, .	2.6	20

#	Article	IF	CITATIONS
73	Impaired regional left ventricular strain after repair of tetralogy of fallot. Journal of Magnetic Resonance Imaging, 2012, 35, 79-85.	3.4	19
74	Negative predictive value and potential cost savings of acute nuclear myocardial perfusion imaging in low risk patients with suspected acute coronary syndrome: A prospective single blinded study. BMC Emergency Medicine, 2009, 9, 12.	1.9	18
75	Infarct quantification using 3D inversion recovery and 2D phase sensitive inversion recovery; validation in patients and ex vivo. BMC Cardiovascular Disorders, 2013, 13, 110.	1.7	16
76	Development and validation of a new automatic algorithm for quantification of left ventricular volumes and function in gated myocardial perfusion SPECT using cardiac magnetic resonance as reference standard. Journal of Nuclear Cardiology, 2011, 18, 874-885.	2.1	15
77	Myocardium at risk can be determined by ex vivo T2-weighted magnetic resonance imaging even in the presence of gadolinium: comparison to myocardial perfusion single photon emission computed tomography. European Heart Journal Cardiovascular Imaging, 2013, 14, 261-268.	1.2	15
78	Peripheral microvascular function is altered in young individuals at risk for hypertrophic cardiomyopathy and correlates with myocardial diastolic function. American Journal of Physiology - Heart and Circulatory Physiology, 2015, 308, H1351-H1358.	3.2	15
79	Validation and development of a new automatic algorithm for time resolved segmentation of the left ventricle in magnetic resonance imaging. Journal of Cardiovascular Magnetic Resonance, 2015, 17, P68.	3.3	15
80	Vortexâ€ring mixing as a measure of diastolic function of the human heart: Phantom validation and initial observations in healthy volunteers and patients with heart failure. Journal of Magnetic Resonance Imaging, 2016, 43, 1386-1397.	3.4	15
81	Longitudinal shortening remains the principal component of left ventricular pumping in patients with chronic myocardial infarction even when the absolute atrioventricular plane displacement is decreased. BMC Cardiovascular Disorders, 2017, 17, 208.	1.7	15
82	A new vessel segmentation algorithm for robust blood flow quantification from twoâ€dimensional phaseâ€contrast magnetic resonance images. Clinical Physiology and Functional Imaging, 2019, 39, 327-338.	1.2	15
83	Short-axis epicardial volume change is a measure of cardiac left ventricular short-axis function, which is independent of myocardial wall thickness. American Journal of Physiology - Heart and Circulatory Physiology, 2010, 298, H530-H535.	3.2	14
84	Longitudinal strain from velocity encoded cardiovascular magnetic resonance: a validation study. Journal of Cardiovascular Magnetic Resonance, 2013, 15, 15.	3.3	14
85	Hydraulic forces contribute to left ventricular diastolic filling. Scientific Reports, 2017, 7, 43505.	3.3	14
86	Isolated pulmonary regurgitation causes decreased right ventricular longitudinal function and compensatory increased septal pumping in a porcine model. Acta Physiologica, 2017, 221, 163-173.	3.8	14
87	Center of volume and total heart volume variation in healthy subjects and patients before and after coronary bypass surgery. Clinical Physiology and Functional Imaging, 2005, 25, 226-233.	1.2	13
88	Identification of residual ischemia, infarction, and microvascular impairment in revascularized myocardial infarction using 64â€slice MDCT. Contrast Media and Molecular Imaging, 2008, 3, 198-206.	0.8	12
89	Intracoronary Injection of Contrast Media Maps the Territory of the Coronary Artery. Academic Radiology, 2008, 15, 1354-1359.	2.5	12
90	Persistent decline in longitudinal and radial strain after coronary microembolization detected on velocity encoded phase contrast magnetic resonance imaging. Journal of Magnetic Resonance Imaging, 2009, 30, 69-76.	3.4	12

#	Article	IF	CITATIONS
91	Effect of oxygen therapy on chest pain in patients with ST elevation myocardial infarction: results from the randomized SOCCER trial. Scandinavian Cardiovascular Journal, 2018, 52, 69-73.	1.2	12
92	Transcatheter closure of atrial septal defect in adults: time-course of atrial and ventricular remodeling and effects on exercise capacity. International Journal of Cardiovascular Imaging, 2019, 35, 2077-2084.	1.5	12
93	Percutaneous transendocardial VEGF gene therapy: MRI guided delivery and characterization of 3D myocardial strain. International Journal of Cardiology, 2010, 143, 255-263.	1.7	11
94	Automatic segmentation of myocardium at risk from contrast enhanced SSFP CMR: validation against expert readers and SPECT. BMC Medical Imaging, 2016, 16, 19.	2.7	11
95	Changes in blood volume shunting in patients with atrial septal defects: assessment of heart function with cardiovascular magnetic resonance during dobutamine stress. European Heart Journal Cardiovascular Imaging, 2017, 18, 1145-1152.	1.2	11
96	Cardiac remodeling in aortic and mitral valve disease: a simulation study with clinical validation. Journal of Applied Physiology, 2019, 126, 1377-1389.	2.5	11
97	Independent validation of metric optimized gating for fetal cardiovascular phaseâ€contrast flow imaging. Magnetic Resonance in Medicine, 2019, 81, 495-503.	3.0	11
98	Disappearance of myocardial perfusion defects on prone SPECT imaging: Comparison with cardiac magnetic resonance imaging in patients without established coronary artery disease. BMC Medical Imaging, 2009, 9, 16.	2.7	10
99	Peak oxygen uptake in relation to total heart volume discriminates heart failure patients from healthy volunteers and athletes. Journal of Cardiovascular Magnetic Resonance, 2010, 12, 74.	3.3	10
100	Coronary microembolization causes long-term detrimental effects on regional left ventricular function. Scandinavian Cardiovascular Journal, 2011, 45, 205-214.	1.2	10
101	A new method for vessel segmentation based on a priori input from medical expertise in cine phase-contrast Magnetic Resonance Imaging. Journal of Cardiovascular Magnetic Resonance, 2014, 16, P355.	3.3	10
102	Effects of oxygen therapy on wallâ€motion score index in patients with <scp>ST</scp> elevation myocardial infarction—the randomized <scp>SOCCER</scp> trial. Echocardiography, 2017, 34, 1130-1137.	0.9	10
103	Preoperative CT of cardiac veins for planning left ventricular lead placement in cardiac resynchronization therapy. Acta Radiologica, 2019, 60, 859-865.	1.1	10
104	High ECG Risk-Scores Predict Late Gadolinium Enhancement on Magnetic Resonance Imaging in HCM in the Young. Pediatric Cardiology, 2021, 42, 492-500.	1.3	10
105	Hemodynamic force analysis is not ready for clinical trials on HFpEF. Scientific Reports, 2022, 12, 4017.	3.3	10
106	Comparison of 1- and 2-day protocols for myocardial SPECT: a Monte Carlo study. Clinical Physiology and Functional Imaging, 2005, 25, 189-195.	1.2	9
107	High-frequency electrocardiogram analysis in the ability to predict reversible perfusion defects during adenosine myocardial perfusion imaging. Journal of Electrocardiology, 2007, 40, 510-514.	0.9	9
108	Coronary artery stenosis in asymptomatic child after arterial switch operation: detection by transthoracic colourâ€flow doppler echocardiography. Acta Paediatrica, International Journal of Paediatrics, 2008, 97, 376-378.	1.5	9

#	Article	IF	CITATIONS
109	Longitudinal left ventricular function is globally depressed within a week of <scp>STEMI</scp> . Clinical Physiology and Functional Imaging, 2018, 38, 1029-1037.	1.2	9
110	Agreement of left ventricular mass in steady state free precession and delayed enhancement MR images: implications for quantification of fibrosis in congenital and ischemic heart disease. BMC Medical Imaging, 2010, 10, 4.	2.7	7
111	Evaluation of the <scp>ECG</scp> based Selvester scoring method to estimate myocardial scar burden and predict clinical outcome in patients with left bundle branch block, with comparison to late gadolinium enhancement <scp>CMR</scp> imaging. Annals of Noninvasive Electrocardiology, 2017, 22, .	1.1	7
112	Simulation of aortopulmonary collateral flow in Fontan patients for use in prediction of interventional outcomes. Clinical Physiology and Functional Imaging, 2018, 38, 622-629.	1.2	7
113	Alterations in ventricular pumping in patients with atrial septal defect at rest, during dobutamine stress and after defect closure. Clinical Physiology and Functional Imaging, 2018, 38, 830-839.	1.2	7
114	The significance of STâ€elevation in aVL in anterolateral myocardial infarction: An assessment by cardiac magnetic resonance imaging. Annals of Noninvasive Electrocardiology, 2018, 23, e12580.	1.1	7
115	Right ventricular remodeling after conduit replacement in patients with corrected tetralogy of Fallot - evaluation by cardiac magnetic resonance. Journal of Cardiothoracic Surgery, 2019, 14, 77.	1.1	7
116	Decreased atrioventricular plane displacement after acute myocardial infarction yields a concomitant decrease in stroke volume. Journal of Applied Physiology, 2020, 128, 252-263.	2.5	7
117	Functional Contribution ofÂCircumferential Versus Longitudinal Strain. Journal of the American College of Cardiology, 2018, 71, 254-255.	2.8	6
118	Cardiac Magnetic Resonance Evaluation of the Extent of Myocardial Injury in Patients with Inferior ST Elevation Myocardial Infarction and Concomitant ST Depression in Leads V1–V3: Analysis from the MITOCARE Study. Cardiology, 2018, 140, 178-185.	1.4	6
119	Changes in left and right ventricular longitudinal function after pulmonary valve replacement in patients with Tetralogy of Fallot. American Journal of Physiology - Heart and Circulatory Physiology, 2020, 318, H345-H353.	3.2	6
120	To what extent are perfusion defects seen by myocardial perfusion SPECT in patients with left bundle branch block related to myocardial infarction, ECG characteristics, and myocardial wall motion?. Journal of Nuclear Cardiology, 2021, 28, 2910-2922.	2.1	6
121	Pulmonary blood volume measured by cardiovascular magnetic resonance: influence of pulmonary transit time methods and left atrial volume. Journal of Cardiovascular Magnetic Resonance, 2021, 23, 123.	3.3	6
122	Computational Fluid Dynamics Support for Fontan Planning in Minutes, Not Hours: The Next Step in Clinical Pre-Interventional Simulations. Journal of Cardiovascular Translational Research, 2022, 15, 708-720.	2.4	6
123	Interdependence between measures of extent and severity of myocardial perfusion defects provided by automatic quantification programs. Nuclear Medicine Communications, 2005, 26, 1125-1130.	1.1	5
124	Coronary flow dynamics in children after repair of Tetralogy of Fallot. International Journal of Cardiology, 2014, 172, 122-126.	1.7	5
125	Intracardiac hemodynamic forces using 4D flow: a new reproducible method applied to healthy controls, elite athletes and heart failure patients. Journal of Cardiovascular Magnetic Resonance, 2016, 18, Q61.	3.3	5
126	Gender but not diabetes, hypertension or smoking affects infarct evolution in ST-elevation myocardial infarction patients – data from the CHILL-MI, MITOCARE and SOCCER trials. BMC Cardiovascular Disorders, 2019, 19, 161.	1.7	5

#	Article	IF	CITATIONS
127	Diagnostic Accuracy Of The Electrocardiographic Decision Support – Myocardial Ischaemia (EDS-MI) Algorithm In Detection Of Acute Coronary Occlusion. European Heart Journal: Acute Cardiovascular Care, 2020, 9, 13-25.	1.0	5
128	Measuring extracellular volume fraction by MRI: First verification of values given by clinical sequences. Magnetic Resonance in Medicine, 2020, 83, 662-672.	3.0	5
129	Valvular imaging in the era of featureâ€tracking: A sliceâ€following cardiac MR sequence to measure mitral flow. Journal of Magnetic Resonance Imaging, 2020, 51, 1412-1421.	3.4	5
130	FourFlow - open source code software for quantification and visualization of time-resolved three-directional phase contrast magnetic resonance velocity mapping. Journal of Cardiovascular Magnetic Resonance, 2012, 14, .	3.3	4
131	Head-to-head comparison of a 2-day myocardial perfusion gated SPECT protocol and cardiac magnetic resonance late gadolinium enhancement for the detection of myocardial infarction. Journal of Nuclear Cardiology, 2013, 20, 797-803.	2.1	4
132	Quantification of left and right atrial kinetic energy using four-dimensional intracardiac magnetic resonance imaging flow measurements. Journal of Cardiovascular Magnetic Resonance, 2013, 15, P218.	3.3	4
133	Validation of an automated method to quantify stress-induced ischemia and infarction in rest-stress myocardial perfusion SPECT. Journal of Nuclear Cardiology, 2014, 21, 503-518.	2.1	4
134	Quantification of myocardial salvage by myocardial perfusion SPECT and cardiac magnetic resonance — reference standards for ECG development. Journal of Electrocardiology, 2014, 47, 525-534.	0.9	4
135	Letter to the Editor: Atrioventricular plane displacement is not the sole mechanism of atrial and ventricular refill. American Journal of Physiology - Heart and Circulatory Physiology, 2015, 309, H1094-H1096.	3.2	4
136	Computerized decision making in myocardial perfusion SPECT: The new era in nuclear cardiology?. Journal of Nuclear Cardiology, 2015, 22, 885-887.	2.1	4
137	Correlation of anteroseptal ST elevation with myocardial infarction territories through cardiovascular magnetic resonance imaging. Journal of Electrocardiology, 2018, 51, 563-568.	0.9	4
138	Discriminatory ability of right atrial volumes with two―and threeâ€dimensional echocardiography to detect elevated right atrial pressure in pulmonary hypertension. Clinical Physiology and Functional Imaging, 2018, 38, 192-199.	1.2	4
139	Chestâ€lead STâ€l amplitudes using arm electrodes as reference instead of the Wilson central terminal in smartphone ECG applications: Influence on STâ€elevation myocardial infarction criteria fulfillment. Annals of Noninvasive Electrocardiology, 2018, 23, e12549.	1.1	4
140	Ischemic QRS prolongation as a biomarker of myocardial injury in STEMI patients. Annals of Noninvasive Electrocardiology, 2019, 24, e12601.	1.1	4
141	Qualitative assessments of myocardial ischemia by cardiac MRI and coronary stenosis by invasive coronary angiography in relation to quantitative perfusion by positron emission tomography in patients with known or suspected stable coronary artery disease. Journal of Nuclear Cardiology, 2020, 27, 2351-2359.	2.1	4
142	Increased pulmonary blood volume variation in patients with heart failure compared to healthy controls: a noninvasive, quantitative measure of heart failure. Journal of Applied Physiology, 2020, 128, 324-337.	2.5	4
143	Quantification of left ventricular contribution to stroke work by longitudinal and radial force-length loops. Journal of Applied Physiology, 2020, 129, 880-890.	2.5	4
144	Myocardial perfusion by CMR coronary sinus flow shows sex differences and lowered perfusion at stress in patients with suspected microvascular angina. Clinical Physiology and Functional Imaging, 2022, 42, 208-219.	1.2	4

#	Article	IF	CITATIONS
145	The impacts on healthcare when coronary angiography as the reference method for diagnostic accuracy of coronary artery disease is replaced by fractional flow reserve!. European Heart Journal, 2017, 38, 999-1001.	2.2	4
146	Comparison of 2D and 4D Flow MRI in Neonates Without General Anesthesia. Journal of Magnetic Resonance Imaging, 2023, 57, 71-82.	3.4	4
147	Diastolic vortex ring formation in the human left ventricle: quantitative analysis using Lagrangian coherent structures and 4D cardiovascular magnetic resonance velocity mapping. Journal of Cardiovascular Magnetic Resonance, 2012, 14, .	3.3	3
148	The shape of the healthy heart is optimized for vortex ring formation. Journal of Cardiovascular Magnetic Resonance, 2016, 18, O23.	3.3	3
149	Gender aspects on exerciseâ€induced ECG changes in relation to scintigraphic evidence of myocardial ischaemia. Clinical Physiology and Functional Imaging, 2018, 38, 798-807.	1.2	3
150	Appropriate coronary revascularization can be accomplished if myocardial perfusion is quantified by positron emission tomography prior to treatment decision. Journal of Nuclear Cardiology, 2021, 28, 1664-1672.	2.1	3
151	Evolution of left ventricular function among subjects with ST-elevation myocardial infarction after percutaneous coronary intervention. BMC Cardiovascular Disorders, 2020, 20, 309.	1.7	3
152	Low diagnostic yield of ST elevation myocardial infarction amplitude criteria in chest pain patients at the emergency department. Scandinavian Cardiovascular Journal, 2021, 55, 145-152.	1.2	3
153	Anterior STEMI associated with decreased strain in remote cardiac myocardium. International Journal of Cardiovascular Imaging, 2021, , 1.	1.5	3
154	Classification of carfentanil synthesis methods based on chemical impurity profile. Forensic Chemistry, 2021, 26, 100355.	2.8	3
155	Ventricular longitudinal function by cardiovascular magnetic resonance predicts cardiovascular morbidity in HFrEF patients. ESC Heart Failure, 2022, 9, 2313-2324.	3.1	3
156	Haemodynamic leftâ€ventricular changes during dobutamine stress in patients with atrial septal defect assessed with magnetic resonance imagingâ€based pressure–volume loops. Clinical Physiology and Functional Imaging, 2022, 42, 422-429.	1.2	3
157	Validation of blood flow partitioning in 4D phase contrast CMR measurements using lagrangian coherent structures. Journal of Cardiovascular Magnetic Resonance, 2011, 13, .	3.3	2
158	Vortex ring mixing in the left ventricle of the human heart. Journal of Cardiovascular Magnetic Resonance, 2013, 15, E27.	3.3	2
159	Whole-heart 4D flow can be acquired with preserved quality without respiratory gating facilitating clinical use. Journal of Cardiovascular Magnetic Resonance, 2015, 17, .	3.3	2
160	Stress-induced ST elevation with or without concomitant ST depression is predictive of presence, location and amount of myocardial ischemia assessed by myocardial perfusion SPECT, whereas isolated stress-induced ST depression is not. Journal of Electrocardiology, 2016, 49, 307-315.	0.9	2
161	Appropriateness of anteroseptal myocardial infarction nomenclature evaluated by late gadolinium enhancement cardiovascular magnetic resonance imaging. Journal of Electrocardiology, 2018, 51, 218-223.	0.9	2
162	Hydraulic force is a novel mechanism of diastolic function that may contribute to decreased diastolic filling in HFpEF and facilitate filling in HFrEF. Journal of Applied Physiology, 2021, 130, 993-1000.	2.5	2

#	Article	IF	CITATIONS
163	Cardiac hypoxic resistance and decreasing lactate during maximum apnea in elite breath hold divers. Scientific Reports, 2021, 11, 2545.	3.3	2
164	Ventricular longitudinal shortening is an independent predictor of death in heart failure patients with reduced ejection fraction. Scientific Reports, 2021, 11, 20280.	3.3	2
165	Pulmonary perfusion and NYHA classification improve after cardiac resynchronization therapy. Journal of Nuclear Cardiology, 2022, 29, 2974-2983.	2.1	2
166	Biventricular Pressure-Volume Loop Assessment Before and After Pulmonary Valve Replacement in Tetralogy of Fallot. Journal of Thoracic Imaging, 2022, 37, W70-W71.	1.5	2
167	Myocardium at risk and myocardial salvage after acute infarction in humans; quantification by magnetic resonance imaging. Journal of Cardiovascular Magnetic Resonance, 2009, 11, .	3.3	1
168	Validation of an algorithm for left ventricular segmentation in 150 patients shows potential for further development towards fully automatic segmentation. Journal of Cardiovascular Magnetic Resonance, 2013, 15, E30.	3.3	1
169	Performance of contrast enhanced SSFP and T2-weighted imaging for determining myocardium at risk in a multi-vendor, multi-center setting- data from the MITOCARE and CHILL-MI trials. Journal of Cardiovascular Magnetic Resonance, 2015, 17, P194.	3.3	1
170	Regional contributions to ventricular stroke volumes are affected on the left side, and not on the right in patients with pulmonary hypertension. Journal of Cardiovascular Magnetic Resonance, 2015, 17, P294.	3.3	1
171	Atrial and ventricular kinetic energy is higher in athletes compared to healthy controls and contributes to improve diastolic filling of the ventricles. Journal of Cardiovascular Magnetic Resonance, 2015, 17, .	3.3	1
172	Phantom validation of 4D flow: independent validation of vortex ring volume quantification using planar laser-induced fluorescence. Journal of Cardiovascular Magnetic Resonance, 2015, 17, P38.	3.3	1
173	Design of clinical cardioprotection trials using CMR: impact of myocardial salvage index and a narrow inclusion window on sample size. Journal of Cardiovascular Magnetic Resonance, 2015, 17, P90.	3.3	1
174	Improvement of computational fluid dynamics simulations of flow in patients with total cavo pulmonary connection and predicting interventional outcomes. Journal of Cardiovascular Magnetic Resonance, 2016, 18, 072.	3.3	1
175	Heart filling exceeds emptying during late ventricular systole in patients with systolic heart failure and healthy subjects – a cardiac MRI study. Clinical Physiology and Functional Imaging, 2019, 39, 192-200.	1.2	1
176	Are biventricular and biatrial function truly preserved after arterial switch operation?. Heart, 2021, 107, 1609-1610.	2.9	1
177	Validation and quantification of left ventricular function during exercise and free breathing from real-time cardiac magnetic resonance images. Scientific Reports, 2022, 12, 5611.	3.3	1
178	Atrioventricular plane displacement and regional function to predict outcome in pulmonary arterial hypertension. International Journal of Cardiovascular Imaging, 2022, 38, 2235-2248.	0.6	1
179	Non-invasive quantification of pressure–volume loops in patients with Fontan circulation. BMC Cardiovascular Disorders, 2022, 22, .	1.7	1
180	Cardiovascular effects of inhaled oxygen assessed with magnetic resonance imaging. Scandinavian Journal of Trauma, Resuscitation and Emergency Medicine, 2009, 17, O9.	2.6	0

#	Article	IF	CITATIONS
181	XMR is a useful modality to guide, map and quantify the perfusion territories of coronary arteries. Journal of Cardiovascular Magnetic Resonance, 2009, 11, .	3.3	0
182	Potential of multidetector computed tomography and magnetic resonance imaging in quantifying left ventricular function, perfusion and viability of chronic microinfarction. Journal of Cardiovascular Magnetic Resonance, 2009, 11, .	3.3	0
183	Myocardium at risk by magnetic resonance imaging: head-to-head comparison of T2-weighted imaging and early gadolinium enhanced steady state free precession. Journal of Cardiovascular Magnetic Resonance, 2012, 14, .	3.3	0
184	Automatic segmentation of myocardium at risk in T2-weighted cardiovascular magnetic resonance. Journal of Cardiovascular Magnetic Resonance, 2012, 14, .	3.3	0
185	Infarct quantification using 3D inversion recovery and 2D phase sensitive inversion recovery, validation in patients and ex vivo. Journal of Cardiovascular Magnetic Resonance, 2012, 14, .	3.3	0
186	Quantification of the contribution of septal movement to stroke volume in healthy subjects, athletes, patients with pulmonary insufficiency and patients with pulmonary hypertension. Journal of Cardiovascular Magnetic Resonance, 2012, 14, .	3.3	0
187	Vortex formation ratio in heart failure compared to healthy volunteers at rest and during exercise. Journal of Cardiovascular Magnetic Resonance, 2013, 15, 065.	3.3	0
188	T2-STIR CMR imaging can be used to assess myocardium at risk with gadolinium present in an experimental setting. Journal of Cardiovascular Magnetic Resonance, 2013, 15, .	3.3	0
189	Infarct size is overestimated by contrast-enhanced CMR in the acute phase but not at 7 days when compared with histopathology. Journal of Cardiovascular Magnetic Resonance, 2014, 16, Ó67.	3.3	0
190	Moderate intensity supine exercise causes decreased cardiac volumes and increased outer volume variations - a cardiac magnetic resonance imaging study. Journal of Cardiovascular Magnetic Resonance, 2014, 16, P38.	3.3	0
191	Left ventricular myocardial perfusion in young patients evaluated for hypertrophic cardiomyopathy at rest and during adenosine hyperemia using cardiac magnetic resonance imaging. Journal of Cardiovascular Magnetic Resonance, 2014, 16, P163.	3.3	0
192	Semi-automatic segmentation of myocardium at risk from contrast enhanced SSFP images - validation against manual delineation and SPECT. Journal of Cardiovascular Magnetic Resonance, 2015, 17, Q127.	3.3	0
193	Phantom validation of 4D flow: independent validation of flow velocity quantification using particle imaging velocimetry. Journal of Cardiovascular Magnetic Resonance, 2015, 17, O18.	3.3	Ο
194	Myocardium at risk quantified by contrast enhanced steady-state free precession does not differ in extent or severity when comparing patients with ST-elevation myocardial infarction treated with standard reperfusion or postconditioning. Journal of Cardiovascular Magnetic Resonance, 2015, 17, P105.	3.3	0
195	Head-to-head comparison of myocardial perfusion SPECT and CMR for assessment of myocardial ischemia. Journal of Cardiovascular Magnetic Resonance, 2015, 17, P119.	3.3	0
196	The extent of myocardium at risk for LAD, RCA and LCx using contrast enhanced SSFP and T2-weighted imaging. Journal of Cardiovascular Magnetic Resonance, 2015, 17, P139.	3.3	0
197	Prediction of appropriate ICD-therapy using infarct heterogeneity from CMR in patients with coronary artery disease. Journal of Cardiovascular Magnetic Resonance, 2015, 17, P165.	3.3	0
198	Hydraulic forces contribute to left ventricular diastolic filling. Journal of Cardiovascular Magnetic Resonance, 2015, 17, P79.	3.3	0

#	Article	IF	CITATIONS
199	Regional adenosine-induced hypoperfusion without hyperenhancement on LGE-MRI in young HCM patients: comparison to subjects at risk of HCM and healthy volunteers. Journal of Cardiovascular Magnetic Resonance, 2015, 17, Q51.	3.3	0
200	Factors determining exercise capacity in patients with atrial septal defect: assessment of heart function with CMR during dobutamine stress. Journal of Cardiovascular Magnetic Resonance, 2015, 17,	3.3	0
201	Alterations in right ventricular pumping in patients with atrial septal defect at rest and during dobutamine stress. Journal of Cardiovascular Magnetic Resonance, 2015, 17, Q86.	3.3	0
202	The evolution of myocardium at risk by T2-STIR MR imaging the first week after acute myocardial ischemia. Journal of Cardiovascular Magnetic Resonance, 2016, 18, P94.	3.3	0
203	Right atrial volume measured by cardiac magnetic resonance correlates with NT-ProBNP and invasive right atrial pressure in pulmonary hypertension, with and without systemic sclerosis. Journal of Cardiovascular Magnetic Resonance, 2016, 18, P300.	3.3	0
204	MR photography of 3D-MR images. Journal of Cardiovascular Magnetic Resonance, 2016, 18, P33.	3.3	0
205	Patients with Tetralogy of Fallot have lower systolic KE in the left ventricle and higher diastolic KE in the right ventricle. Journal of Cardiovascular Magnetic Resonance, 2016, 18, P184.	3.3	0
206	New automatic algorithm for segmentation of myocardial scar in both inversion recovery and phase sensitive inversion recovery late gadolinium enhancement: validation against TTC and in multi-center, multi-vendor patient data. Journal of Cardiovascular Magnetic Resonance, 2016, 18, P221.	3.3	0
207	Patients with Cardiac syndrome X have decreased global myocardial perfusion compared to gender matched controls; insights from CMR coronary sinus flow measurements. Journal of Cardiovascular Magnetic Resonance, 2016, 18, P240.	3.3	0
208	Automated time-resolved tracking algorithm of the atrioventricular plane displacement in CMR images. Journal of Cardiovascular Magnetic Resonance, 2016, 18, P43.	3.3	0
209	Myocardial perfusion using cardiac magnetic resonance: Evidence of decreased global myocardial perfusion in patients with systemic sclerosis with possible gender differences. Journal of Cardiovascular Magnetic Resonance, 2016, 18, P71.	3.3	0
210	The Authors Reply:. JACC: Cardiovascular Imaging, 2016, 9, 1016-1017.	5.3	0
211	Response by Jablonowski et al to Letter Regarding Article, "Cardiovascular Magnetic Resonance to Predict Appropriate Implantable Cardioverter Defibrillator Therapy in Ischemic and Nonischemic Cardiomyopathy Patients Using Late Gadolinium Enhancement Border Zone: Comparison of Four Analvsis Methodsâ€t Circulation: Cardiovascular Imaging, 2018, 11, e007333.	2.6	0
212	Regional contributions to left ventricular stroke volume determined by cardiac magnetic resonance imaging in cardiac resynchronization therapy. BMC Cardiovascular Disorders, 2021, 21, 519.	1.7	0